Bull. Mater. Sci., Vol. 38, No. 5, September 2015, pp. 1135–1139. © Indian Academy of Sciences.

Facile hydrothermal synthesis of CeO_2 nanopebbles

N SABARI ARUL[1,2], D MANGALARAJ[2] and JEONG IN HAN[1,*]

[1]Department of Chemical and Biochemical Engineering, Dongguk University-Seoul, 100715 Seoul, South Korea
[2]Department of Nanoscience and Technology, Bharathiar University, Coimbatore 641 046, India

MS received 17 October 2014; accepted 13 April 2015

Abstract. Cerium oxide (CeO_2) nanopebbles have been synthesized using a facile hydrothermal method. X-ray diffraction pattern (XRD) and transmission electron microscopy analyses confirm the presence of CeO_2 nanopebbles. XRD shows the formation of cubic fluorite CeO_2 and the average particle size estimated from the Scherrer formula was found to be 6.69 nm. X-ray absorption spectrum of CeO_2 nanopebbles exhibits two main sharp white lines at 880 and 898 eV due to the spin orbital splitting of M_4 and M_5. Optical absorption for the synthesized CeO_2 nanopebbles exhibited a blue shift (E_g = 3.35 eV) with respect to the bulk CeO_2 (E_g = 3.19 eV), indicating the existence of quantum confinement effects.

Keywords. CeO_2; nanopebbles; structural; XAS; quantum confinement effect.

1. Introduction

Shape-controlled synthesis of nanomaterials has been attracting remarkable significant interest in various applications owing to their unique structural, optical and electronic properties.[1,2] Cerium oxide (CeO_2) is one of the most abundant rare earth oxides with a wide bandgap (3.2 eV) and has attracted significant interest in many applications in technological fields, including three-way catalytic,[3] sunscreen,[4] solid oxide fuel cells,[5] biomedical,[6] photocatalyst[7] and UV blocking materials.[8] Moreover, significant effort has been made to fabricate CeO_2 nanomaterials with precise size and morphology.[9,10] Several methods have been employed to synthesize CeO_2 nanostructures, including nanotubes,[11] nanorods,[12] nanowires,[13] nanocubes[14] and quantum dots.[15] Among all nanoconstructions, CeO_2 nanostructures with cubic shape can exploit nanocrystals packing and generate a great compact structure with mainly exposure of six homogeneous (100) crystal facets.[16,17] Moreover, the advantages of synthesizing CeO_2 nanopebbles with cubic shape exhibit exceptional reducibility and high oxygen storage capacity, representing they are potential catalytic materials.[18–20] However, to the best of our knowledge the reports on the synthesis of CeO_2 nanopebbles via the hydrothermal method are limited up to date.

Herein, we report a facile hydrothermal synthesis of CeO_2 nanopebbles and its quantum confinement effect. In this study, we have adopted a hydrothermal method for obtaining CeO_2 nanopebbles because it has various advantages over the other methods, such as eco-friendly, cost-effective, versatile size and shape control of nanostructures and reproducibility.[21] The obtained CeO_2 nanopebbles are characterized using X-ray diffraction (XRD), field-emission scanning electron microscope (FESEM), transmission electron microscopy (TEM), energy-dispersive X-ray analysis (EDAX), selected-area electron diffraction (SAED), X-ray absorption spectroscopy (XAS) and UV−visible spectroscopy. From the optical properties, quantum confinement effects of the synthesized CeO_2 nanopebbles were investigated.

2. Experimental

2.1 *Synthesis of CeO_2 nanopebbles*

All chemicals used in the experiment were of analytical grade and were used without further purification. Initially, required amount of $CeCl_3 \cdot 7H_2O$ was dissolved in deionized water and subsequently 3 M of NaOH solution was added dropwise into the starting solution under vigorous stirring. After ultrasonic treatment for 30 min, the solution was transferred into Teflon autoclave and maintained at 180°C for 24 h. Then the autoclave was cooled down naturally to room temperature. The obtained products were centrifuged, washed several times with distilled water and absolute ethanol, dried under vacuum at 90°C for overnight, and collected for characterization.

2.2 *Characterization*

The crystal structure of the synthesized CeO_2 nanopebbles was determined by using a PAN Analytical

*Author for correspondence (hanji@dongguk.edu)

X'Pert pro diffractometer with CuKα radiation (λ = 0.1540 nm) with a scanning rate of 0.05 s^{-1}. EDAX and SAED were also recorded in the TEM with an accelerating voltage of 200 kV. XAS measurements were performed at 111D-1 spherical grating monochromator beam line of Canadian light source. The total energy resolution was 100 meV and the spectra were measured at 20 K. The base pressure of the XAS chamber was in the range of 10^{-8} Pa. A Shimadzu UV−visible spectrophotometer-3600 was used to investigate the optical properties.

3. Results and discussion

Figure 1a shows the XRD spectrum of CeO_2 nanopebbles synthesized at 180°C for 24 h. The XRD peaks along the (111), (200), (220), (311) and (222) planes confirm that the cubic fluorite structure of CeO_2 matches well with JCPDS PDF no. 34-0394. The average crystallite sizes estimated from the Scherrer formula by using the (111) plane of CeO_2 is found to be 6.69 nm. The estimated lattice parameter of the synthesized product is found to be 0.542 nm, which is slightly higher than bulk CeO_2 (0.541 nm). The increase in the lattice expansion in small particles is due to the increased oxygen vacancies.[22]

Furthermore, an alternative analysis Raman spectroscopy was investigated to confirm the crystalline quality of CeO_2 nanopebbles. Figure 1b shows a Raman F_{2g} band at 465 cm^{-1}, which is attributed to the Raman active vibration mode of cubic structure. The Raman band at 600 cm^{-1} is related to the oxygen vacancies due to the presence of Ce^{3+} in the CeO_2 lattice and also defects caused by small size effects.[23]

TEM analysis was performed to get a clear insight into the microstructure of CeO_2 nanopebbles. Figure 2a–d shows the TEM images of the CeO_2 nanopebbles. The size of individual CeO_2 nanopebbles was observed to be ~100 nm. Figure 2e shows the high-resolution TEM images having lattice fringes with spacing of 0.311 nm, which is inconsistent with the line spacing of the (111) planes of cubic fluorite CeO_2 (JCPDS PDF no. 34-0394). The average nanoparticle size (~7 nm) of CeO_2 observed by TEM result was in good agreement with the XRD results. The inset image of figure 2e depicts the SAED pattern for the obtained CeO_2 nanopebbles, indicating the polycrystalline nature of the CeO_2 and are consistent with XRD data (figure 1a).

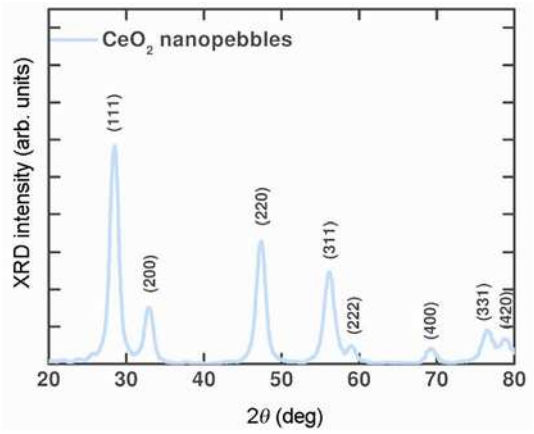

Figure 1. X-ray diffraction spectra of CeO_2 nanopebbles.

Yang and Gao[14] have reported that the smaller and larger nanocubes are predominantly grown by the Ostwald ripening and oriented attachment process, respectively. In the hydrothermal process after the nucleation stage, where the small nanocrystals are dissolved or re-precipitated to grow the larger crystals by the Ostwald ripening process, resulting in the formation of CeO_2 nanopebbles.[24] Figure 2f shows the elemental composition of the CeO_2 nanopebbles, it was found to be 70.84 wt% of Ce, 12.39 wt% of Cu (grid), 4.03 wt% of C (carbon coating), 12.75 wt% of O and no other impurities were observed.

Figure 3a shows the XAS spectra in the M-edge region of CeO_2 nanopebbles gives the information in the initial state of 4f occupancy. The XAS spectra of CeO_2 exhibits two main sharp white lines at 880 and 898 eV due to the spin orbital splitting of $3d_{3/2} \rightarrow 4f_{5/2}$ (M_4) and $3d_{5/2} \rightarrow 4f_{7/2}$ (M_5). The relative intensities of the white lines were used to determine the valence of cerium ions.[25] The measurement of the ratio of M_5/M_4 is close to 1.31 if the particle size is less than ~3 nm, and the valence of cerium ions is 3^+ throughout the particle.[26] Whereas the M_5/M_4 ratio is close to 0.91 for the larger particles (~15 nm) and the valence of those cerium ions is 4^+ state.[26] In our case, the valence of cerium ions will be mainly 4^+ state, because the estimated particle size of CeO_2 nanopebbles is greater than 3 nm. Figure 3b shows the oxygen K-edge XAS spectra is attributed to O 2p states mixing with Ce 3d–O 2p.

Figure 4a shows the optical absorption spectra of the synthesized CeO_2 nanopebbles. The optical absorption spectra showed a strong UV-absorption band below 350 nm, resulting from the charge-transfer transitions from the O 2p to Ce 4f in O^{2-} and Ce^{4+} states.[14] The relation between the absorption coefficient (α) and the incident photon energy ($h\nu$) can be written as follows:

$$(\alpha h\nu) = A(h\nu - E_g)^n, \quad (1)$$

where A is a constant value, E_g the bandgap of the material, h Planck's constant, ν the frequency of the incident radiation and n is 0.5 for directly allowed transitions. The optical bandgaps of the CeO_2 nanopebbles have been determined by using equation (1). Figure 4b shows the $(\alpha h\nu)^2$ *vs.* $h\nu$ plot of CeO_2 nanopebbles. The optical bandgap of the synthesized CeO_2 nanopebbles (E_g = 3.35 eV) is blue-shifted when compared to those of bulk CeO_2

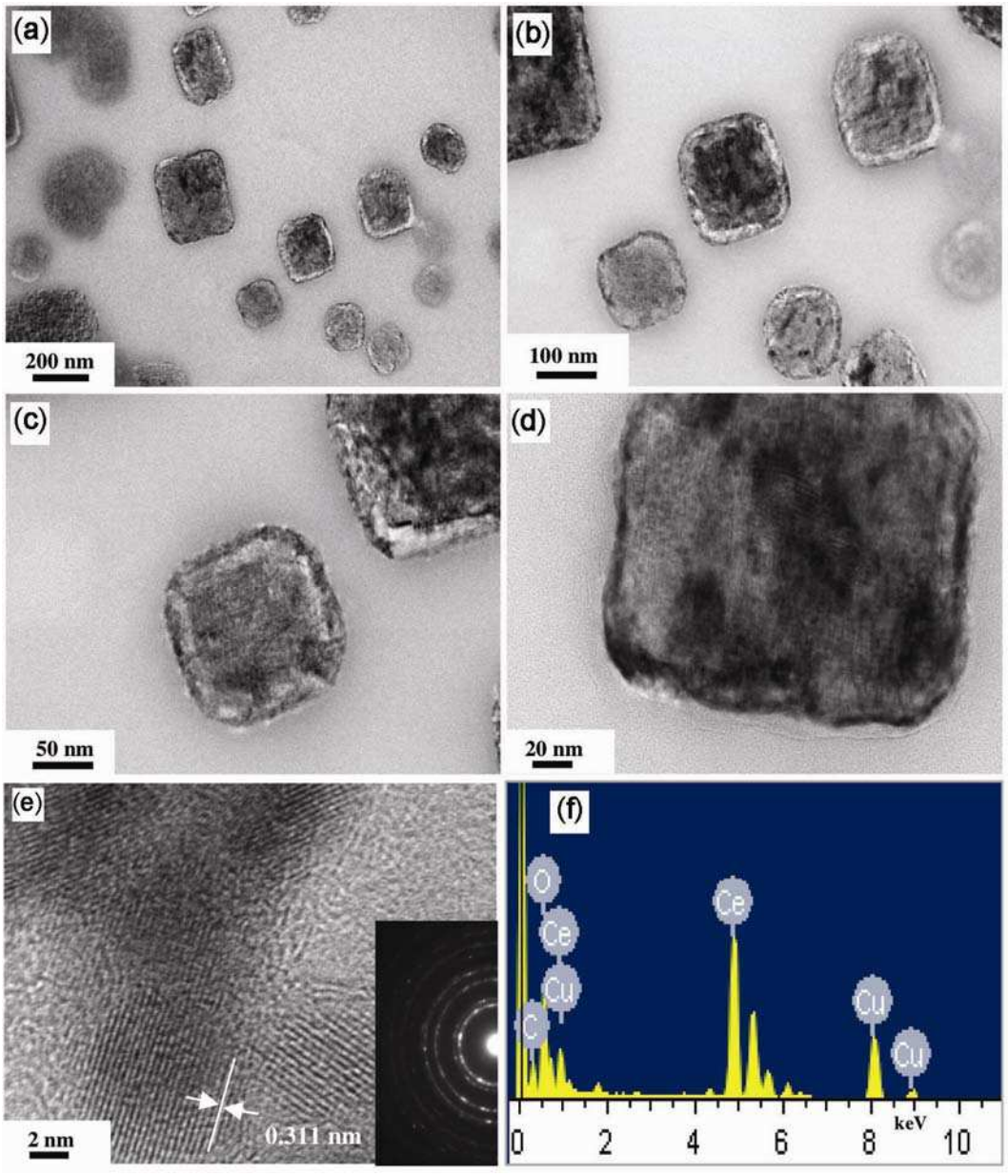

Figure 2. (**a**)–(**e**) TEM images and (**f**) EDAX spectrum of CeO_2 nanopebbles.

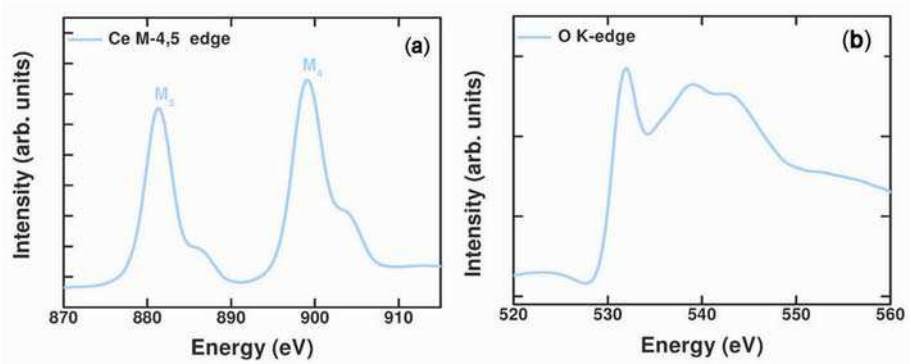

Figure 3. Synchrotron spectra of CeO_2 nanopebbles, (**a**) Ce M-edge XAS and (**b**) O K-edge XAS.

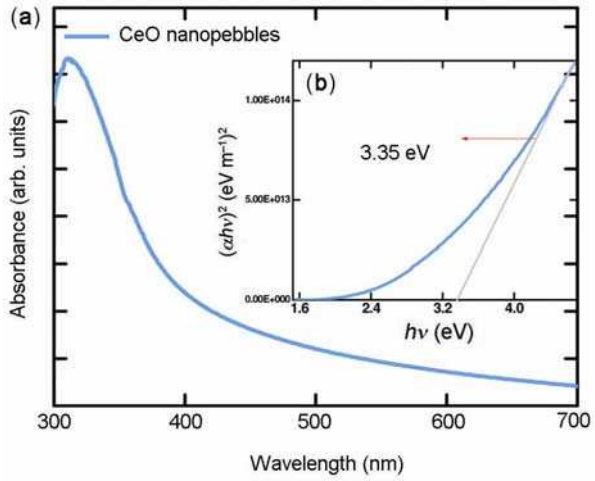

Figure 4. (**a**) UV–visible absorbance spectra and (**b**) plot of $(\alpha h\nu)^2$ *vs.* $h\nu$ of CeO_2 nanopebbles.

(E_g = 3.19 eV). The semi-empirical equation,[27] elucidates the quantitative analysis of CeO_2 bandgap energy for direct transition on the particle size

$$E_{g(nano)} = E_{g(bulk)} + \frac{\hbar^2\pi^2}{2R^2}\left[\frac{1}{m_e} + \frac{1}{m_h}\right] - \frac{1.8e^2}{\varepsilon R}, \qquad (2)$$

where $E_{g(nano)}$ is the measured bandgap width of CeO_2 nanoparticles, $E_{g(bulk)}$ the bandgap width for the crystalline CeO_2, $\hbar$ the Planck constant, R the nanoparticle radius, μ the reduced mass and m_e and m_h are effective masses of electron (m_e/m_h = 0.42 for CeO_2) in the conduction band and holes in valance band, respectively, e the electron charge and ε the relative dielectric constant (~24) value of CeO_2. The estimated particle diameter of the CeO_2 nanopebbles is found to be 6.8 nm, which is less than Bohr radius of CeO_2 (7–8 nm). Ho *et al*[28] have reported similar bandgap value of ceria nanoparticle to be 3.36 eV with a particle diameter of 7.6 nm.[28] Thus, the size of the synthesized CeO_2 nanoparticle is smaller than Bohr radius, which is strong enough to cause a quantum confinement effect in obtaining CeO_2 nanoparticles.[29]

4. Conclusions

In summary, CeO_2 nanopebbles were synthesized by a surfactant-free facile hydrothermal method. XRD, TEM and XAS analyses confirm the presence of cubic fluorite-type CeO_2 nanopebbles. XRD spectra showed the presence of cubic phase of CeO_2 and the average particle size estimated from the Scherrer formula was 6.69 nm. XAS spectrum of CeO_2 nanopebbles showed two main sharp white lines at 880 and 898 eV due to the spin orbital splitting of $3d_{3/2} \rightarrow 4f_{5/2}$ (M_4) and $3d_{5/2} \rightarrow 4f_{7/2}$ (M_5). The optical bandgap energy of CeO_2 nanopebbles exhibited a blue shift (E_g = 3.35 eV) with respect to its bulk counterparts (E_g = 3.19 eV) due to the quantum confinement effect. Our results indicate that the CeO_2 nanopebbles have great potential use in photocatalyst, gas sensor and solar cell applications.

Acknowledgements

NSA thanks Bharathiar University for providing University Research Fellowship. He also thanks A Dhayal Raj, Department of Physics, Bharathiar University, Coimbatore and Q Yang, Department of Mechanical Engineering, University of Saskatchewan, Saskatoon, Canada, for assistance with XAS analysis. This work was supported by the Technology Innovation Program (10041957, Design and Development of fibre-based flexible display) funded by the Ministry of Trade, Industry and Energy (MI, Korea) and Civil-Military Technology Cooperation Center (13-DU-EE-13).

References

1. Campbell C T and Peden C H F 2005 *Science* **309** 713
2. Tsunekawa S, Ishikawa K, Li Z Q, Kawazoe Y and Kasuya Y 2000 *Phys. Rev. Lett.* **85** 3440
3. Liu G F, Wang Q Y, Zhao B, Shen M Q and Zhou R X 2011 *J. Hazard. Mater.* **186** 911
4. Imanaka N, Masui T, Hirai H and Adachi G 2003 *Chem. Mater.* **15** 2289
5. Atkinson A, Barnett S, Gorte R J, Irvine J T S, McEvoy A J, Mogensen M B, Singhal S and Vohs J M 2004 *Nat. Mater.* **3** 17
6. Chen J, Patil, Seal S and McGinnis J G 2006 *Nat. Nanotechnol.* **1** 142
7. Chen F J, Cao Y L and Jia D Z 2011 *Appl. Surf. Sci.* **257** 9226
8. Masui T, Yamamoto M, Sakata T, Mori H and Adachi G Y 2000 *J. Mater. Chem.* **10** 353
9. Rovira L G, Amaya J M, Haro M L, Rio E D, Hungria A B, Midgley P, Calvino J J, Bernal S and Botana F J 2009 *Nano Lett.* **9** 1395
10. Yuan Q, Duan H H, Li L L, Li Z X, Duan W T, Zhang L S, Song W G and Yan C H 2010 *Adv. Mater.* **22** 1475
11. Zhang D, Fu H, Shi L, Fang J and Li Q 2007 *J. Solid State Chem.* **180** 654
12. Zhou K, Wang X, Sun X, Peng Q and Li Y 2005 *J. Catal.* **229** 206
13. Wu L, Wiesmann H J, Moodenbaugh A R, Klie R F, Zhu Y, Welch D O and Suenaga M 2004 *Phys. Rev.* **B69** 125415
14. Yang S and Gao L 2006 *J. Am. Chem. Soc.* **128** 9330
15. Lehnen T, Schlafer J, Mathur S and Anorg Z 2014 *Anorg. Allg. Chem.* **640** 819
16. Deori K, Gupta D, Saha B and Deka S 2014 *ACS Catal.* **4** 3169
17. Yang Z, Yang Y, Liang H and Liu L 2009 *Mater. Lett.* **63** 1774

18. Yang Z, Zhou K, Liu X, Tian Q, Lu D and Yang S 2007 *Nanotechnology* **18** 185606
19. Nguyena T D, Dinha C T, Mrabet D, Tran-Thi M N and Doa T O 2013 *J. Colloid Interface Sci.* **394** 100
20. Zhang Y C, Lei M, Huang K, Liang C, Wang Y J, Ding S S, Zhang R, Fan D Y, Yang H J and Wang Y G 2014 *Mater. Lett.* **116** 46
21. Mai H X, Sun L D, Zhang Y W, Si R, Feng W, Zhang H P, Liu H C and Yan C H 2005 *J. Phys. Chem. B* **109** 24380
22. Zhang F, Chan S W, Spanier J E, Apak E, Jin Q, Robinson R D and Herman I P 2002 *Appl. Phys. Lett.* **80** 127
23. Liyanage A D, Perera S D, Tan K, Chabal Y and Balkus K J 2014 *ACS Catal.* **4** 577
24. Taniguchi T, Katsumata K, Omata S, Okada K and Matsushita N 2011 *Cryst. Growth Des.* **11** 3754
25. Niewa R, Hu Z, Grazioli C, Robler U, Golden M S, Knupfer M, Fink J, Giefers H, Wortmann G, de Groot F M F and DiSalvo F J 2002 *J. Alloys Compd.* **346** 129
26. Wu G S, Xie T, Yuan X Y, Cheng B C and Zhang L D 2004 *Mater. Res. Bull.* **39** 1023
27. Zhang F, Jin Q and Chan S W 2004 *J. Appl. Phys.* **95** 4319
28. Ho C, Yu J C, Kwong T, Mak A C and Lai S 2005 *Chem. Mater.* **17** 4514
29. Tsunekawa S, Fukuda T and Kasuya A 2000 *J. Appl. Phys.* **87** 1318